Atmos. Chem. Phys., 15, 11571–11592, 2015
www.atmos-chem-phys.net/15/11571/2015/
doi:10.5194/acp-15-11571-2015

Atmospheric Chemistry and Physics Open Access EGU

Granger causality from changes in level of atmospheric CO_2 to global surface temperature and the El Niño–Southern Oscillation, and a candidate mechanism in global photosynthesis

L. M. W. Leggett and D. A. Ball

Global Risk Policy Group Pty Ltd, Townsville, Queensland, Australia

Correspondence to: L. M. W. Leggett (mleggett.globalriskprogress@gmail.com)

Received: 3 May 2014 – Published in Atmos. Chem. Phys. Discuss.: 21 November 2014
Revised: 13 September 2015 – Accepted: 30 September 2015 – Published: 21 October 2015

Abstract. A significant difference, now of some 16 years' duration, has been shown to exist between the observed global surface temperature trend and that expected from the majority of climate simulations. For its own sake, and to enable better climate prediction for policy use, the reasons behind this mismatch need to be better understood. While an increasing number of possible causes have been proposed, the candidate causes have not yet converged.

With this background, this paper reinvestigates the relationship between change in the level of CO_2 and two of the major climate variables, atmospheric temperature and the El Niño–Southern Oscillation (ENSO).

Using time-series analysis in the form of dynamic regression modelling with autocorrelation correction, it is shown that first-difference CO_2 leads temperature and that there is a highly statistically significant correlation between first-difference CO_2 and temperature. Further, a correlation is found for second-difference CO_2 with the Southern Oscillation Index, the atmospheric-pressure component of ENSO. This paper also shows that both these correlations display Granger causality.

It is shown that the first-difference CO_2 and temperature model shows no trend mismatch in recent years.

These results may contribute to the prediction of future trends for global temperature and ENSO.

Interannual variability in the growth rate of atmospheric CO_2 is standardly attributed to variability in the carbon sink capacity of the terrestrial biosphere. The terrestrial biosphere carbon sink is created by the difference between photosynthesis and respiration (net primary productivity): a major way of measuring global terrestrial photosynthesis is by means of satellite measurements of vegetation reflectance, such as the Normalized Difference Vegetation Index (NDVI). In a preliminary analysis, this study finds a close correlation between an increasing NDVI and the increasing climate model/temperature mismatch (as quantified by the difference between the trend in the level of CO_2 and the trend in temperature).

1 Introduction

Understanding current global climate requires an understanding of trends both in Earth's atmospheric temperature and the El Niño–Southern Oscillation (ENSO), a characteristic large-scale distribution of warm water in the tropical Pacific Ocean and the dominant global mode of year-to-year climate variability (Holbrook et al., 2009). However, despite much effort, the average projection of current climate models has become statistically significantly different from the 21st century global surface temperature trend (Fyfe et al., 2013; Fyfe and Gillett, 2014) and has failed to reflect the statistically significant evidence that annual-mean global temperature has not risen in the 21st century (Fyfe et al., 2013; Kosaka and Shang-Ping, 2013).

The situation is illustrated visually in Fig. 1 which shows the increasing departure over recent years of the global surface temperature trend from that projected by a representative mid-range global climate model (GCM) for global surface temperature – the CMIP5, RCP4.5 scenario model (Taylor et al., 2012).

It is noted that recent studies have reconsidered the correct quantification of this model–observation difference: they re-

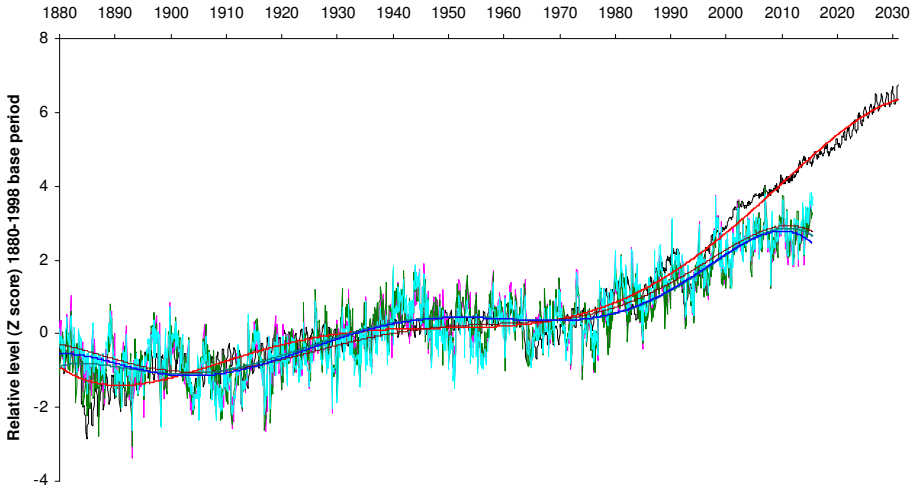

Figure 1. Monthly data, *Z*-scored to aid visual comparison (see Sect. 1). To show their core trends for illustrative purposes, the four series are fitted with sixth-order polynomials. Shown are: the output of an IPCC mid-range scenario model (CMIP5, RCP4.5 scenario) run for the IPPC fifth assessment report (IPCC, 2014) (black curve)(polynomial fit (pn): red curve). Global surface temperature data sets: HadCRUT4 (purple curve) (pn: blue curve); Cowtan and Way (2014) (green curve) (pn: light green curve); Karl et al. (2015) (aquamarine curve) (pn: brown curve).

port analysis suggesting that it is in effect less evident (Cowtan and Way, 2014; Karl et al., 2015).

The effect of these alternative quantifications on the model–observation difference is also shown in Fig. 1.

Figure 1 shows the departure over recent years of a standard time series of temperature (HadCRUT4) from that projected by a representative mid-range global climate model (GCM) for global surface temperature – the CMIP3, SRESA1B scenario model (Meehl et al., 2007). The figure also shows the alternative temperature series (Cowtan and Way, 2014; Karl et al., 2015).

Figure 1 shows that the alternative quantifications reduce the scale of the difference seen using HadCRUT4 but do not eliminate it.

It is noted that the level of atmospheric CO_2 is a good proxy for the International Panel on Climate Change (IPCC) models predicting the global surface temperature trend: according to IPCC (2014), on decadal to interdecadal timescales and under continually increasing effective radiative forcing, the forced component of the global surface temperature trend responds to the forcing trend relatively rapidly and almost linearly.

Turning to ENSO, the extremes of its variability cause extreme weather events (such as floods and droughts) in many regions of the world. Modelling provides a wide range of predictions for future ENSO variability, some showing an increase, others a decrease, and some no change (Guilyardi et al., 2012; Bellenger et al., 2014).

A wide range of physical explanations has now been proposed for the global warming slowdown. These involve proposals either for changes in the way the radiative mechanism itself is working or for the increased influence of other physical mechanisms. Chen and Tung (2014) place these proposed explanations into two categories. The first involves a reduction in radiative forcing: by a decrease in stratospheric water vapour, an increase in background stratospheric volcanic aerosols, by 17 small volcano eruptions since 1999, increasing coal-burning in China, the indirect effect of time-varying anthropogenic aerosols, a low solar minimum, or a combination of these. The second category of candidate explanation involves planetary sinks for the excess heat. The major focus for the source of this sink has been physical and has involved ocean heat sequestration. However, evidence for the precise nature of the ocean sinks is not yet converging: according to Chen and Tung (2014) their study followed the original proposal of Meehl et al. (2011) that global deep-ocean heat sequestration is centred on the Pacific. However, their observational results were that such deep-ocean heat sequestration is mainly occurring in the Atlantic and the Southern oceans.

Alongside the foregoing possible physical causes, Hansen et al. (2013) have suggested that the mechanism for the pause in the global temperature increase since 1998 might be the planetary biota, in particular the terrestrial biosphere: that is (IPCC, 2007), the fabric of soils, vegetation and other biological components, the processes that connect them and the carbon, water and energy that they store.

It is widely considered that the interannual variability in the growth rate of atmospheric CO_2 is a sign of the operation of the influence of the planetary biota.

Again, IPCC (2007) states the following: “the atmospheric CO_2 growth rate exhibits large interannual variations. The change in fossil fuel emissions and the estimated variability in net CO_2 uptake of the oceans are too small to account

for this signal, which must be caused by year-to-year fluctuations in land–atmosphere fluxes."

In the IPCC Fourth Assessment Report, Denman et al. (2007) state (italics denote present author emphasis): "Interannual and inter-decadal variability in the growth rate of atmospheric CO_2 is dominated by the *response of the land biosphere to climate variations*. ... The terrestrial biosphere *interacts strongly with the climate*, providing both positive and negative feedbacks due to biogeophysical and biogeochemical processes. ... Surface climate is determined by the balance of fluxes, which can be changed by radiative (e.g. albedo) or non-radiative (e.g. water-cycle-related processes) terms. Both radiative and non-radiative terms *are controlled by details of vegetation*."

Denman et al. (2007) also note that many studies have confirmed that the variability of CO_2 fluxes is mostly due to land fluxes, and that tropical lands contribute strongly to this signal. A predominantly terrestrial origin of the growth rate variability can be inferred from (1) atmospheric inversions assimilating time series of CO_2 concentrations from different stations, (2) consistent relationships between $\delta^{13}CO_2$ and CO_2, (3) ocean model simulations and (4) terrestrial carbon cycle and coupled model simulations. For one prominent estimate carried out by the Global Carbon Project, the land sink is calculated as the residual of the sum of all sources minus the sum of the atmosphere and ocean sinks (Le Quéré et al., 2014).

The activity of the land sink can also be estimated directly. The terrestrial biosphere carbon sink is created by photosynthesis: a major way of measuring global land photosynthesis is by means of satellite measurements of potential photosynthesis from greenness estimates. The measure predominantly used is the Normalized Difference Vegetation Index (NDVI) (Running et al., 2004; Zhang et al., 2014). NDVI data are available from the start of satellite observations in 1980 to the present. For this period the trend signature in NDVI has been shown to correlate closely with that for atmospheric CO_2 (Barichivich et al., 2013). This noted, we have not been able to find studies which have compared NDVI data with the difference between climate model outputs and temperature.

2 Methodological issues and objectives of the study

2.1 Methodological issues

Before considering further material, it is helpful now to consider a range of methodological issues and concepts. The first concept is to do with the notion of causality.

According to Hidalgo and Sekhon (2011) there are four prerequisites to enable an assertion of causality. The first is that the cause must be prior to the effect. The second prerequisite is "constant conjunction" between variables (Hume, 1751, cited in Hidalgo and Sekhon, 2011). This relates to the degree of fit between variables. The final requirements are those concerning manipulation and random placement into experimental and control categories. It is noted that each of the four prerequisites is necessary but not sufficient on its own for causality.

With regard to the last two criteria, the problem for global studies such as global climate studies is that manipulation and random placement into experimental and control categories cannot be carried out.

One method using correlational data, however, approaches more closely the quality of information derived from random placement into experimental and control categories. The concept is that of Granger causality (Granger, 1969). According to Stern and Kaufmann (2014), a time-series variable "x" (e.g. atmospheric CO_2) is said to "Granger-cause" variable "y" (e.g. surface temperature) if past values of x help to predict the current level of y, better than just the past values of y do, given all other relevant information.

Reference to the above four aspects of causality will be made to help structure the review of materials in the following sections.

2.2 Objectives of the study

What has been considered to influence the biota's creation of the pattern observed in the trend in the growth rate of atmospheric CO_2? The candidates for the influences on the biota have mainly been considered in prior research to be atmospheric variations, primarily temperature and/or ENSO (e.g. Kuo et al., 1990; Wang et al., 2013). Despite its proposed role in global warming overall, CO_2 (in terms of the initial state of atmospheric CO_2 exploited by plants at time A) has not generally been isolated and studied in detail through time-series analysis as an influence in the way the biosphere influences the CO_2 left in the atmosphere at succeeding time B.

This lack of attention to the influence of the biosphere on climate variables seems to have come about for two reasons, one concerning ENSO, the other, temperature. For ENSO, the reason is that the statistical studies are unambiguous that ENSO leads rate of change of CO_2 (e.g. Lean and Rind, 2008). On the face of it, therefore, this ruled out CO_2 as the first mover of the ecosystem processes. For temperature, the reason was that the question of whether atmospheric temperature leads rate of change of CO_2 or vice versa is less settled.

In the first published study on this question, Kuo et al. (1990) provided evidence that the signature of interannual atmospheric CO_2 (measured as its first difference) fitted temperature (passing therefore one of the four tests for causality, of close conjunction).

The relative fits of both the level of and change in the level of atmospheric CO_2 (measured as its first difference) with global surface temperature up to the present are depicted in Fig. 2. Attention is drawn to both signature (fine-grained data structure) and, by means of polynomial smoothing, core trend for each data series.

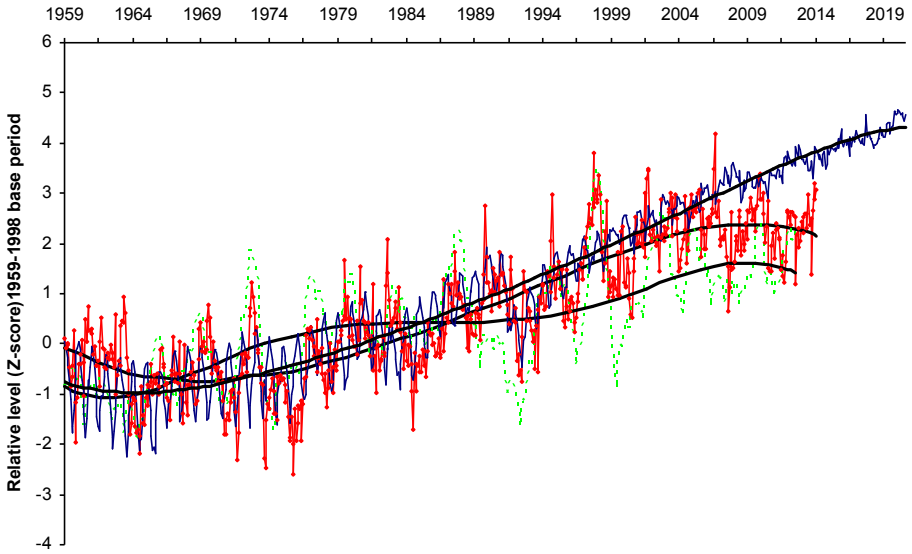

Figure 2. *Z*-scored monthly data: observed global surface temperature (green dashed curve) compared with that projected from an IPCC mid-range scenario global climate model (GCM) – the CMIP3, SRESA1B scenario run for the IPCC fourth assessment report (IPCC, 2007) (blue curve). Also shown is the trend in first-difference atmospheric CO_2 (smoothed by two 13-month moving averages) (red dotted curve). To show their core trends for illustrative purposes, the three series are fitted with fifth-order polynomials.

Concerning signature, while clearly first-difference CO_2 and temperature are not identical, each is more alike than either is to the temperature model based on the level of CO_2. As well, the polynomial fits show that the same likeness groupings exist for core trend.

Kuo et al. (1990) also provided evidence concerning another of the causality prerequisites – priority. This was that the signature of first-difference CO_2 *lagged* temperature (by 5 months). This idea has been influential. More recently, Adams and Piovesan (2005) noted that climate variations acting on ecosystems are believed to be responsible for variation in CO_2 increment, but there are major uncertainties in identifying processes, including uncertainty concerning *instantaneous* (present authors' emphasis) versus lagged responses. Wang et al. (2013) observed that the strongest coupling is found between the CO_2 growth rate and the *concurrent* (present authors' emphasis) tropical land temperature. Wang et al. (2013) nonetheless state in their conclusion that the strong temperature–CO_2 coupling they observed is best explained by the additive responses of tropical terrestrial respiration and primary production to temperature variations, which reinforce each other in enhancing *temperature's control* (present author emphasis) on tropical net ecosystem exchange.

Another perspective on the relative effects of rising atmospheric CO_2 concentrations on the one hand and temperature on the other has been provided by extensive direct experimentation on plants. In a large-scale meta-analysis of such experiments, Dieleman et al. (2012) drew together results on how ecosystem productivity and soil processes responded to combined warming and CO_2 manipulation, and compared it with those obtained from single-factor CO_2 and temperature manipulation. While the meta-analysis found that responses to combined CO_2 and temperature treatment showed the greatest effect, this was only slightly larger than for the CO_2-only treatment. By contrast, the effect of the CO_2-only treatment was markedly larger than for the warming-only treatment.

In looking at leading and lagging climate series more generally, the first finding of correlations between the rate of change (in the form of the first-difference) of atmospheric CO_2 and a climate variable was with the foregoing and the Southern Oscillation Index (SOI) component of ENSO (Bacastow, 1976). Here evidence was presented that the SOI led first-difference atmospheric CO_2. There have been further such studies (see Imbers et al., 2013, for overview) which, taken together, consistently show that the highest correlations are achieved with SOI leading temperature by some months (3–4 months).

In light of the foregoing, this paper reanalyses by means of time-series regression analysis which of first-difference CO_2 and temperature lead. The joint temporal relationship between interannual atmospheric CO_2, global surface temperature and ENSO (indicated by the SOI) is also investigated.

The foregoing also shows that a strong case can be made for further investigating the planetary biota, influenced by atmospheric CO_2, as a candidate influence on (cause of) climate outcomes. This question is also explored in this paper.

A number of Granger causality studies have been carried out on climate time series (see review in Attanasio et al., 2013). We found six papers which assessed atmospheric CO_2

and global surface temperature (Sun and Wang, 1996; Triacca, 2005; Kodra et al., 2011; Attanasio and Triacca, 2011; Attanasio et al., 2013; Stern and Kaufmann, 2014). Of these, while all but one (Triacca, 2005) found Granger causality, it was not with CO_2 concentration as studied in this paper but with CO_2 radiative forcing ($\ln CO_2$, Attanasio and Triacca, 2011).

As well, all studies used annual rather than monthly data. For Granger causality analysis, the data series used must display the statistical property of stationarity (see Sect. 3: Data and methods). Such annual data for each of atmospheric CO_2 and temperature are not stationary of themselves but must be transformed into a new, stationary series by differencing (Sun and Wang, 1996). Further, data at this level of aggregation can "mask" correlational effects that only become apparent when higher-frequency (e.g. monthly) data are used.

Rather than using a formal Granger causality analysis, a number of authors have instead used conventional multiple regression models in attempts to quantify the relative importance of natural and anthropogenic influencing factors on climate outcomes such as global surface temperature. These regression models use contemporaneous explanatory variables. For example, see Lean and Rind (2008, 2009); Foster and Rahmstorf (2011); Kopp and Lean (2011); Zhou and Tung (2013). This type of analysis effectively assumes a causal direction between the variables being modelled. It is incapable of providing a proper basis for testing for the presence or absence of causality. In some cases account has been taken of autocorrelation in the model's errors, but this does not overcome the fundamental weakness of standard multiple regression in this context. In contrast, Granger causality analysis that we adopt in this paper provides a formal testing of both the presence and direction of this causality (Granger 1969).

From such multiple regression studies, a common set of main influencing factors (also called explanatory or predictor variables) has emerged. These are (Lockwood, 2008; Folland et al., 2013; Zhou and Tung, 2013): El Niño–Southern Oscillation (ENSO), or Southern Oscillation Index (SOI) alone; volcanic aerosol optical depth; total solar irradiance; and the trend in anthropogenic greenhouse gas (the predominant anthropogenic greenhouse gas being CO_2). In these models, ENSO/SOI is the factor embodying interannual variation. Imbers et al. (2013) show that a range of different studies using these variables have all produced similar and close fits with the global surface temperature.

With this background, this paper first presents an analysis concerning whether the first-difference of atmospheric CO_2 leads or lags global surface temperature. After assessing this, questions of autocorrelation, strength of correlation, and of causality are then explored. Given this exploration of correlations involving first-difference atmospheric CO_2, the possibility of the correlation of second-difference CO_2 with climate variables is also explored.

Correlations are assessed at a range of timescales to seek the time extent over which relationships are held, and thus whether they are a special case or possibly longer term in nature. The timescales involved are, using instrumental data, over two periods starting, respectively, from 1959 and 1877; and, using paleoclimate data, over a period commencing from 1515. The correlations are assessed by means of regression models explicitly incorporating autocorrelation using dynamic modelling methods. Granger causality between CO_2 and, respectively, temperature and SOI is also explored. Atmospheric CO_2 rather than emissions data are used, and where possible at monthly rather than annual aggregation. Finally, as noted, we have not been able to find studies which have compared the gap between climate models and temperature with NDVI data, so an assessment of this question is carried out. All assessments were carried out using the time-series statistical software packages Gnu Regression, Econometrics and Time-series Library (GRETL) (available from: http://gretl.sourceforge.net/, accessed 23 January 2014) and IHS Eviews (IHS EViews 2011).

3 Data and methods

We present results of time-series analyses of climate data. The data assessed are global surface temperature, atmospheric carbon dioxide (CO_2) and the Southern Oscillation Index (SOI). The regressions are presented in several batches based on the length of data series for which the highest temporal resolution is available. The first batch of studies involves the data series for which the available high resolution series is shortest: this is for atmospheric carbon dioxide (CO_2) and commences in 1958. These studies are set at monthly resolution.

The second batch of studies is for data able to be set at monthly resolution not involving CO_2. These studies begin with the time point at which the earliest available monthly SOI data commences, 1877.

The final batch of analyses utilises annual data. These studies use data starting variously in the 16th or 18th centuries.

Data from 1877 and more recently are from instrumental sources; earlier data are from paleoclimate sources. Data from the mid-range outputs of two climate models are also used.

For instrumental data sources for global surface temperature, we used the Hadley Centre–Climate Research Unit combined land SAT and SST (HadCRUT) version 4.2.0.0 (Morice et al., 2012), for atmospheric CO_2, the US Department of Commerce National Oceanic and Atmospheric Administration Earth System Research Laboratory Global Monitoring Division Mauna Loa, Hawaii, monthly CO_2 series (Keeling et al., 2009), and for volcanic aerosols the National Aeronautic and Space Administration Goddard Institute for Space Studies Stratospheric Aerosol Optical Thick-

ness series (Sato et al., 1993). Southern Oscillation Index data (Troup, 1965) are from the Science Delivery Division of the Department of Science, Information Technology, Innovation and the Arts (DSITIA), Queensland, Australia. Solar irradiance data are from J. Lean (personal communication, 2012).

With regard to the El Niño–Southern Oscillation, according to IPCC (2014) the term El Niño was initially used to describe a warm-water current that periodically flows along the coast of Ecuador and Peru, disrupting the local fishery. It has since become identified with a basin-wide warming of the tropical Pacific Ocean east of the dateline. This oceanic event is associated with a fluctuation of a global-scale tropical and subtropical surface atmospheric pressure pattern called the Southern Oscillation. This atmosphere–ocean phenomenon is coupled, with typical timescales of 2 to about 7 years, and known as the El Niño–Southern Oscillation (ENSO).

The El Niño (temperature) component of ENSO is measured by changes in the sea surface temperature of the central and eastern equatorial Pacific relative to the average temperature. The Southern Oscillation (atmospheric pressure) ENSO component is often measured by the surface pressure anomaly difference between Tahiti and Darwin.

For the present study we choose the SOI atmospheric pressure component rather than the temperature component of ENSO to stand for ENSO as a whole. This is because it is considered to be more valid to conduct an analysis in which temperature is an outcome (dependent variable) without also having temperature as an input (independent variable). The correlation between SOI and the other ENSO indices is high, so we believe this assumption is robust.

Palaeoclimate data sources are: atmospheric CO_2, from 1500 – ice cores (Robertson et al., 2001); (NH) temperature, from 1527 – tree ring data (Moberg et al., 2005); SOI, from 1706 – tree ring data (Stahle et al., 1998).

Normalized Difference Vegetation Index (NDVI) monthly data from 1980 to 2006 are from the GIMMS (Global Inventory Modeling and Mapping Studies) data set (Tucker et al., 2005). NDVI data from 2006 to 2013 were provided by the Institute of Surveying, Remote Sensing and Land Information, University of Natural Resources and Life Sciences, Vienna. Data series projected from two representative mid-range global climate models (GCMs) for global surface temperature were used. Series were from the CMIP3, SRESA1B scenario model (Meehl et al., 2007) and the CMIP5, RCP4.5 scenario model (Taylor et al., 2012).

Statistical methods used are standard (Greene, 2012). Categories of methods used are normalisation; differentiation (approximated by differencing); and time-series analysis. Within time-series analysis, methods used are smoothing; leading or lagging of data series relative to one another to achieve best fit; assessing a prerequisite for using data series in time-series analysis, that of stationarity; including autocorrelation in models by use of dynamic regression models; and investigating causality by means of a multivariate time-series model, known as a vector autoregression (VAR) and its associated Granger causality test. These methods will now be described in turn.

To make it easier to assess the relationship between the key climate variables visually, the data were normalised using statistical Z scores or standardised deviation scores (expressed as "relative level" in the figures). In a Z-scored data series, each data point is part of an overall data series that sums to a zero mean and variance of 1, enabling comparison of data having different native units. Hence, when several Z-scored time series are depicted in a graph, all the time series will closely superimpose, enabling visual inspection to clearly discern the degree of similarity or dissimilarity between them.

Individual figure legends contain details on the series lengths.

In the time-series analyses, SOI and global atmospheric surface temperature are the dependent variables. We tested the relationship between each of these variables and (1) the change in atmospheric CO_2 and (2) the variability in its rate of change. We express these CO_2-related variables as finite differences. The finite differences used here are of both the first- and second-order types (we label these "first" and "second" differences in the text). Variability is explored using both intra-annual (monthly) data and interannual (yearly) data. The period covered in the figures is shorter than that used in the data preparation because of the loss of some data points due to calculations of differences and of moving averages.

Smoothing methods are used to the degree needed to produce similar amounts of smoothing for each data series in any given comparison. Notably, to achieve this outcome, series resulting from higher levels of differences require more smoothing. Smoothing is carried out initially by means of a 13-month moving average – this also minimises any remaining seasonal effects. If further smoothing is required, then this is achieved by taking a second moving average of the initial moving average (to produce a double moving average) (Hyndman, 2010). Often, this is performed by means of a further 13-month moving average to produce a 2×13-month moving average. For descriptive statistics to describe the long-term variation of a time-series trend, polynomial smoothing is sometimes used.

It is important to consider what effects this filtering of our data may have on the ensuing statistical analysis. In these analyses, only the CO_2 series was smoothed and therefore requires assessment. To do this, we tested if the smoothed (2×13-month moving average) first-difference CO_2 series used here has different key dynamics to that of the original raw (unsmoothed) data from which the smoothed series was derived. Lagged correlogram analysis showed that the maximum, and statistically significant, correlation of the smoothed series with the unsmoothed series occurs when there is no phase shift. This suggests that the particular smoothing used should provide no problems in the assess-

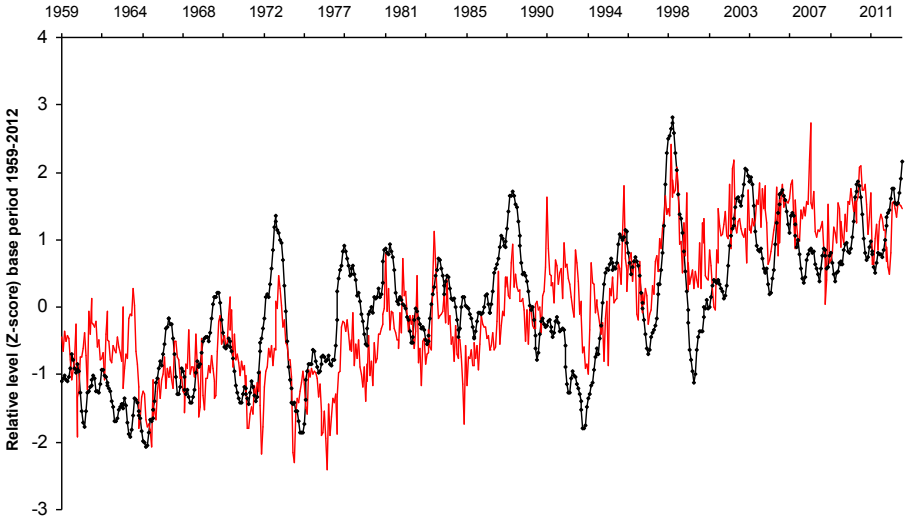

Figure 3. *Z*-scored monthly data: global surface temperature (red curve) compared to first-difference atmospheric CO_2 smoothed by two 13-month moving averages (black dotted curve).

ment of which of first-difference CO_2 and temperature has priority.

Second, there is extensive evidence that while the effect of seasonal adjustment (via smoothing) on the usual tests for unit roots in time-series data is to reduce their power in small samples, this distortion is *not* an issue with samples of the size used in this study (see e.g. Ghysels, 1990; Franses, 1991; Ghysels and Perron, 1993; Diebold, 1993). Moreover, Olekalns (1994) shows that seasonal adjustment by using dummy variables also impacts adversely on the finite-sample power of these tests, so there is little to be gained by considering this alternative approach. Finally, one of the results emerging from the Granger causality literature is that while such causality can be "masked" by the smoothing of the data, apparent causality cannot be "created" from non-causal data. For example, see Sims (1971), Wei (1982), Christiano and Eichenbaum (1987), Marcellino (1999), Breitung and Swanson (2002) and Gulasekaran and Abeysinghe (2002).

Finally, seasonally adjusting the data by a range of alternative approaches did not qualitatively change the results discussed in the paper. The results of these assessments are given in the Supplement.

This means that our results relating to the existence of Granger causality should not be affected adversely by the smoothing of the data that has been undertaken.

Variables are led or lagged relative to one another to achieve best fit. These leads or lags were determined by means of time-lagged correlations (correlograms). The correlograms were calculated by shifting the series back and forth relative to each other, 1 month at a time.

With this background, the convention used in this paper for unambiguously labelling data series and their treatment after smoothing or leading or lagging is depicted in the following example. The atmospheric CO_2 series is transformed into its first difference and smoothed twice with a 13-month moving average. The resultant series is then *Z*-scored. This is expressed as Z2x13mma1stDiffCO_2.

Note that to assist readability in text involving repeated references, atmospheric CO_2 is sometimes referred to simply as CO_2 and global surface temperature as temperature.

The time-series methodology used in this paper involves the following procedures.

First, any two or more time series being assessed by time-series regression analysis must be what is termed stationary in the first instance, or be capable of transformed into a new stationary series (by differencing). A series is stationary if its properties (mean, variance, covariances) do not change with time (Greene, 2012). The (augmented) Dickey–Fuller test is applied to each variable. For this test, the null hypothesis is that the series has a unit root, and hence is non-stationary. The alternative hypothesis is that the series is integrated of order zero.

Second, the residuals from any time-series regression analysis then conducted must not be significantly different from white noise. This is done seeking correct model specification for the analysis.

After Greene (2012) it is noted that the results of standard ordinary least squares (OLS) regression analysis assume that the errors in the model are uncorrelated. Autocorrelation of the errors violates this assumption. This means that the OLS estimators are no longer the best linear unbiased estimators (BLUE). Notably and importantly this does not bias the OLS coefficient estimates. However statistical significance can be overestimated, and possibly greatly so, when the autocorrelations of the errors at low lags are positive.

Table 1. Lag of first-difference CO_2 relative to surface temperature series for global, tropical, Northern Hemisphere and Southern Hemisphere categories.

	Lag in months of first-difference CO_2 relative to global surface temperature category
Hadcrut4SH	−1
Hadcrut4Trop	−1
Hadcrut4_nh	−3
Hadcrut4Glob	−2

Addressing autocorrelation can take either of two alternative forms: *correcting for it* (for example, for first-order autocorrelation by the Cochrane–Orcutt procedure), or *taking it into account*.

In the latter approach, the autocorrelation is taken to be a consequence of an inadequate specification of the temporal dynamics of the relationship being estimated. The method of dynamic modelling (Pankratz, 1991) addresses this by seeking to explain the current behaviour of the dependent variable in terms of both contemporaneous and past values of variables. In this paper the dynamic modelling approach is taken.

To assess the extent of autocorrelation in the residuals of the initial non-dynamic OLS models run, the Breusch–Godfrey procedure is used. Dynamic models are then used to take account of such autocorrelation. To assess the extent to which the dynamic models achieve this, Kiviet's Lagrange multiplier F test (LMF) statistic for autocorrelation (Kiviet, 1986) is used.

Hypotheses related to Granger causality (see Introduction) are tested by estimating a multivariate time-series model, known as a vector autoregression (VAR), for level of and first-difference CO_2 and other relevant variables. The VAR models the current values of each variable as a linear function of their own past values and those of the other variables. Then we test the hypothesis that x does not cause y by evaluating restrictions that exclude the past values of x from the equation for y and vice versa.

Stern and Kander (2011) observe that Granger causality is not identical to causation in the classical philosophical sense, but it does demonstrate the likelihood of such causation or the lack of such causation more forcefully than does simple contemporaneous correlation. However, where a third variable, z, drives both x and y, x might still appear to drive y though there is no actual causal mechanism directly linking the variables (any such third variable must have some plausibility – see Sect. 5).

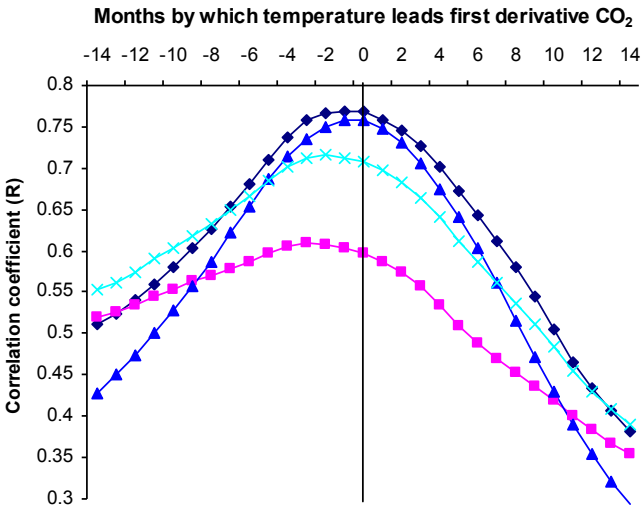

Figure 4. Correlograms of first-difference CO_2 with surface temperature for global (turquoise curve with crosses), tropical (blue curve with triangles), Northern Hemisphere (purple curve with boxes) and Southern Hemisphere (black curve with diamonds) categories.

4 Results

4.1 Relationship between first-difference CO_2 and temperature

4.1.1 Priority

Figure 2 shows that, while clearly first-difference CO_2 and temperature are not identical in signature, each is more alike than either is to the temperature model based on the level of CO_2. As well, the figure shows that the same likeness relationships exist for the core trend. The purpose of the forthcoming sections is to see the extent to which these impressions are statistically significant.

The first question assessed is that of priority: which of first-difference atmospheric CO_2 and global surface temperature leads the other? The two series are shown for the period 1959 to 2012 in Fig. 3.

To quantify the degree of difference in phasing between the variables, time-lagged correlations (correlograms) were calculated by shifting the series back and forth relative to each other, 1 month at a time. These correlograms are given in Fig. 4 for global and regional data. For all four relationships shown, first-difference CO_2 always leads temperature. The leads differ as quantified in Table 1.

It is possible for a lead to exist overall on average but for a lag to occur for one or other specific subsets of the data. This question is explored in Fig. 5 and Table 2. Here the full 1959–2012 period of monthly data – some 640 months – for each of the temperature categories is divided into three approximately equal sub-periods, to provide 12 correlograms. It can be seen that in all 12 cases, first-difference CO_2 leads

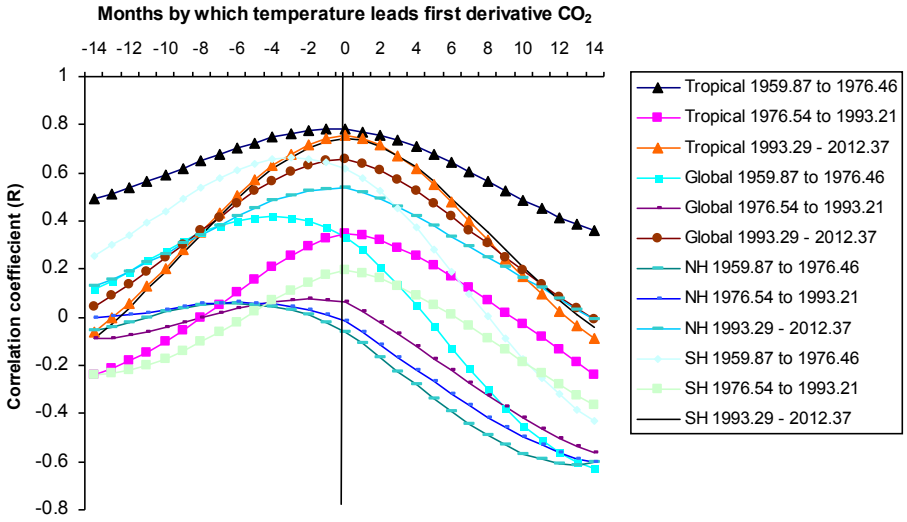

Figure 5. Correlograms of first-difference CO_2 with surface temperature for global, tropical, Northern Hemisphere and Southern Hemisphere categories, each for three time-series sub-periods.

Table 2. Lag of first-difference CO_2 relative to surface temperature series for global, tropical, Northern Hemisphere and Southern Hemisphere categories, each for three time-series sub-periods.

Temperature category	Time period	Lag of first-difference CO_2 relative to global surface temperature series
NH	1959.87 to 1976.46	−6
NH	1976.54 to 1993.21	−6
Global	1959.87 to 1976.46	−4
SH	1959.87 to 1976.46	−3
Global	1976.54 to 1993.21	−2
Tropical	1959.87 to 1976.46	0
Tropical	1976.54 to 1993.21	0
Tropical	1993.29 to 2012.37	0
Global	1993.29 to 2012.37	0
NH	1993.29 to 2012.37	0
SH	1976.54 to 1993.21	0
SH	1993.29 to 2012.37	0

temperature. It is also noted that earlier sub-periods tend to display longer first-difference CO_2 leads. For the most recent sub-period the highest correlation is when the series are neither led nor lagged.

4.1.2 Correspondence between first-difference CO_2 and global surface temperature curves

The second prerequisite for causality, close correspondence, is also seen between first-difference CO_2 and global surface temperature in Fig. 3.

4.1.3 Time series analysis

Both first-difference CO_2 being shown to lead temperature, and the two series displaying close correspondence, are considered a firm basis for the time-series analysis of the statistical relationship between first-difference CO_2 and temperature which follows. For this further analysis, we choose global surface temperature as the temperature series because, while its maximum correlation with first-difference CO_2 is not the highest (Fig. 5), its global coverage by definition is greatest. (In this section, TEMP stands for global surface temperature (HadCRUT4), and other block capital terms are variable names used in the modelling.)

The order of integration, denoted $I(d)$, is an important characteristic of a time series. It reports the minimum number of differences required to obtain a covariance stationary series. As stated above, all series used in a time-series regression must be series which are stationary without further differencing (Greene, 2012); that is, display an order of integration of $I(0)$. If a series has an order of integration greater than zero, it can be transformed by appropriate differencing into a new series which is stationary.

By means of the augmented Dickey–Fuller (ADF) test for unit roots, Table 3 provides the information concerning stationarity for the level of, and first-difference of, CO_2, as well as for global surface temperature. Test results are provided for both monthly and annual data. The test was applied with an allowance for both a drift and deterministic trend in the data, and the degree of augmentation in the Dickey–Fuller regressions was determined by minimising the Schwartz information criterion.

The results show that for both the monthly and annual series used, the variables TEMP and FIRST-DIFFERENCE CO_2 are stationary ($I(0)$); but the level of CO_2 is not. The

Table 3. Augmented Dickey–Fuller (ADF) tests for stationarity of unit roots in both monthly and annual data 1969 to 2012 for level of atmospheric CO_2, first-difference CO_2 and global surface temperature.

	Monthly data				Annual data			
	ADF statistic*	p value	Order of integration	Test interpretation	ADF statistic*	p value	Order of integration	Test interpretation
Level of CO_2	−0.956	0.9481	$I(1)$	Non-stationary	−0.309	0.991	$I(1)$	Non-stationary
First-difference CO_2	−17.103	5.72×10^{-54}	$I(0)$	Stationary	−4.319	0.003	$I(0)$	Stationary
Temp	−5.115	0.00011	$I(0)$	Stationary	−3.748	0.019	$I(0)$	Stationary

* The Dickey–Fuller regressions allowed for both drift and trend; the augmentation level was chosen by minimising the Schwartz information criterion.

level of CO_2 is shown to be $I(1)$ because (Table 3) its first-difference is stationary.

In contrast, Beenstock et al. (2012), using annual data, report that their series for the level of atmospheric CO_2 forcing is an $I(2)$ variable and therefore is stationary in *second* differences. To reconcile these two results, we refer to Pretis and Hendry (2013), who reviewed Beenstock et al. (2012). Pretis and Hendry (2013) take issue with the finding of $I(2)$ for the anthropogenic forcings studied – including CO_2 – and find evidence that this finding results from the combination of two different data sets measured in different ways which make up the 1850–2011 data set which Beenstock et al. (2012) test. Regarding this composite series, Pretis and Hendry (2013) write the following:

"In the presence of these different measurements exhibiting structural changes, a unit-root test on the entire sample could easily not reject the null hypothesis of $I(2)$ even when the data are in fact $I(1)$. Indeed, once we control for these changes, our results contradict the findings in Beenstock et al. (2012)."

Pretis and Hendry (2013) give their results for CO_2 in their Table 1. Note that in the table, the level of CO_2 data are transformed into first-difference data (Beenstock et al., 2012, claim the *level* of CO_2 is $I(2)$; if that is the case, the first-difference of the level of CO_2 that Pretis and Hendry, 2013, should find would be $I(1)$).

Pretis and Hendry (2013) also state the following:

"Unit-root tests are used to determine the level of integration of time series. Rejection of the null hypothesis provides evidence against the presence of a unit-root and suggests that the series is $I(0)$ (stationary) rather than $I(1)$ (integrated).

... based on augmented Dickey–Fuller (ADF) tests (see Dickey and Fuller, 1981), the first-difference of annual radiative forcing of CO_2 is stationary initially around a constant (over 1850–1957), then around a linear trend (over 1958–2011). Although these tests are based on sub-samples corresponding to the shift in the measurement system, there is sufficient power to reject the null hypothesis of a unit root."

Hence for annual data Pretis and Hendry (2013) find first-difference CO_2 to be stationary – $I(0)$, not $I(1)$ – as is found in this study (Table 3).

With this question of the order of integration of the time series considered, we now turn to the next step of the time-series analysis. As Table 3, above, and Pretis and Hendry (2013) show, the variable of the level of CO_2 is non-stationary (specifically, integrated of order one, i.e. $I(1)$). Attempting to assess TEMP in terms of the level of CO_2 would result in an "unbalanced regression", as the dependent variable (TEMP) and the explanatory variable (CO_2) have different orders of integration. It is well-known (e.g. Banerjee et al., 1993, pp. 190–191, and the references therein) that in unbalanced regressions the t statistics are biased away from zero; that is, one can appear to find statistically significant results when in fact they are not present. In fact, this occurrence of spurious significance is found when we regress TEMP on CO_2. This is strong evidence that any analysis should involve the variables TEMP and FIRST-DIFFERENCE CO_2, and not TEMP and CO_2.

For TEMP and FIRST-DIFFERENCE CO_2, one must next assess the extent to which autocorrelation affects the time-series model. This is done by obtaining diagnostic statistics from an OLS regression. This regression shows, by means of the Breusch–Godfrey test for autocorrelation (up to order 12 – that is, including all monthly lags up to 12 months), that there is statistically significant autocorrelation at lags of 1 and 2 months, leading to an overall Breusch–Godfrey test statistic (LMF) = 126.901, with p value $= P(F(12, 626) > 126.901) = 1.06 \times 10^{-158}$.

Autocorrelation is a consequence of an inadequate specification of the temporal dynamics of the relationship being estimated. With this in mind, a dynamic model (Greene, 2012) with two lagged values of the dependent variable as additional independent variables has been estimated. Results are shown in Table 4. The LMF test shows that there is now no statistically significant unaccounted-for autocorrelation, thus supporting the use of this dynamic model specification. Table 4 shows that a highly statistically significant model has been established. First it shows that the temperature in a given period is strongly influenced by the temperature of closely preceding periods (see Sect. 5 for a possible mechanism for this). Further, it provides evidence that there is also a clear, highly statistically significant role in the model for first-difference CO_2.

Table 4. OLS dynamic regression between first-difference atmospheric CO_2 and global surface temperature for monthly data for the period 1959–2012, with autocorrelation taken into account

Independent variable/s[a]	Dependent variable[a]	Independent variable regression coefficients	Independent variable p value	Whole model adjusted R-squared	Whole model p value	LM test for autocorrelation[b]
Led2mx13mma1stdiff CO_2	TEMP	0.097	< 0.00001	0.861	6.70×10^{-273}	0.144
Led1mTEMP		0.565	< 0.00001			
Led2mTEMP		0.306	< 0.00001			

[a] Z-scored. [b] Whole model: Lagrange multiplier (LM) test for autocorrelation up to order 12 – null hypothesis: no autocorrelation.

Table 5. Pairwise correlations (correlation coefficients (R)) between selected climate variables.

	2x13mmafirstdiff CO_2	Hadcrut4Global	3x13mma2nddiffCO_2
Hadcrut4Global	0.7	1	
3x13mma2nddiffCO_2	0.06	−0.05	1
13mmaReverseSOI	0.25	0.14	0.37

4.1.4 Granger causality analysis

We now can turn to assessing if first-difference atmospheric CO_2 may not only correlate with, but also contribute causatively to, global surface temperature. This is done by means of Granger causality analysis.

Recalling that both TEMP and FIRST-DIFFERENCE CO_2 are stationary, it is appropriate to test the null hypothesis of no Granger causality from FIRST-DIFFERENCE CO_2 to TEMP by using a standard vector autoregressive (VAR) model without any transformations to the data. The Akaike information criterion (AIC) and the Schwartz information criterion (SIC) were used to select an optimal maximum lag length (k) for the variables in the VAR. This lag length was then lengthened, if necessary, to ensure that:

i. the estimated model was dynamically stable (i.e. all of the inverted roots of the characteristic equation lie inside the unit circle);

ii. the errors of the equations were serially independent.

The relevant EViews output from the VAR model is entitled VAR Granger causality/block exogeneity Wald tests and documents the following summary results – Wald statistic (p value): null depicts that there is no Granger causality from FIRST-DIFFERENCE CO_2 to TEMP; number of lags $K = 4$; chi-square 26.684 (p value = 0.000). A p value of this level is highly statistically significant and means the null hypothesis of no Granger causality is very strongly rejected; that is, over the period studied there is strong evidence that FIRST-DIFFERENCE CO_2 Granger-causes TEMP.

We recognise that as temperature is stationary, while CO_2 is not, these two variables cannot correlate in the usual sense. However, given that Granger non-causality tests can have low power due to the presence of lagged dependent variables, it is sensible to seek support, or confirmation, for the result just discussed. This can be done by testing for Granger non-causality between the levels of CO_2 and TEMP. In this case, the testing procedure must be modified to allow for the differences in the orders of integration of the data series.

Once again, the levels of both series are used. For each VAR model, the maximum lag length (k) is determined, but then one additional lagged value of both TEMP and CO_2 is included in each equation of the VAR. However, the Wald test for Granger non-causality is applied only to the coefficients of the original k lags of CO_2. Toda and Yamamoto (1995) show that this modified Wald test statistic will still have an asymptotic distribution that is chi-square, even though the level of CO_2 is non-stationary. Here the relevant Wald Statistic (p value): null depicts that there is no Granger causality from level of CO_2 to TEMP; number of lags $K = 4$; chi-square 2.531 (p value = 0.470). The lack of statistical significance indicated by the p value is strong confirmation that level of CO_2 does not Granger-cause TEMP.

With the above two assessments done, it is significant that with regard to global surface temperature we are able to discount causality involving the level of CO_2, but establish causality involving first-difference CO_2.

4.2 Relationship between second-difference CO_2 and temperature and Southern Oscillation Index

4.2.1 Priority and correspondence

Given the results of this exploration of correlations involving first-difference atmospheric CO_2, the possibility of the correlation of second-difference CO_2 with climate variables is also explored. The climate variables assessed are global surface

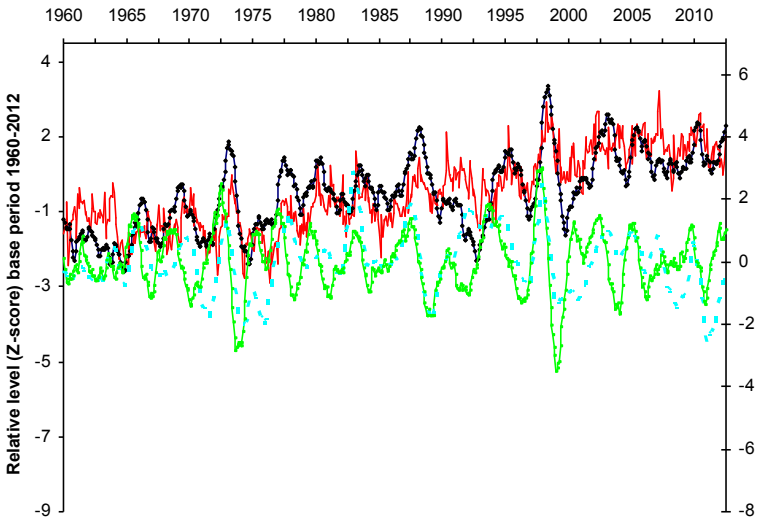

Figure 6. *Z* scored monthly data: global surface temperature (red curve) and first-difference atmospheric CO_2 smoothed by two 13-month moving averages (black dotted curve) (left-hand scale); sign-reversed SOI smoothed by a 13-month moving average (blue dashed curve) and second-difference atmospheric CO_2 smoothed by three 13-month moving averages (green barred curve) (right-hand scale).

Table 6. Pairwise correlations (correlation coefficients (R)) between selected climate variables, phase-shifted as shown in the table.

	Led2m2x13mmafirstdiffCO_2	Hadcrut4Global	Led4m3x13mma2nddiffCO_2
Hadcrut4Global	0.71	1	
Led4m3x13mma2nddiffCO_2	0.23	0.09	1
13mmaReverseSOI	0.16	0.14	0.49

temperature and the Southern Oscillation Index (SOI). In this section, data are from the full period for which monthly instrumental CO_2 data are available, 1958 to the present. For this period, the series neither led nor lagged appear as follows (Fig. 6). For the purpose of this figure, to facilitate depiction of trajectory, second-difference CO_2 (left axis) and SOI (right axis) are offset so that all four curves display a similar origin in 1960.

Figure 6 shows that, alongside the close similarity between first-difference CO_2 and temperature already demonstrated, there is a second apparent distinctive pairing between second-difference CO_2 and SOI. The figure shows that the overall trend, amplitude and phase – the signature – of each pair of curves is both matched within each pair and different from the other pair. The remarkable sorting of the four curves into two groups is readily apparent. Each pair of results provides context for the other – and highlights the different nature of the other pair of results.

Recalling that (even uncorrected for any autocorrelation) correlational data still hold information concerning regression coefficients, we initially use OLS correlations without assessing autocorrelation to provide descriptive statistics. Table 5 includes, without any phase-shifting to maximise fit, the six pairwise correlations arising from all possible combinations of the four variables other than with themselves. Here it can be seen that the two highest correlation coefficients (in bold in the table) are firstly between first-difference CO_2 and temperature, and secondly between second-difference CO_2 and SOI.

In Table 6, phase shifting has been carried out to maximise fit (shifts shown in the titles of the variables in the table). This results in an even higher correlation coefficient for second-difference CO_2 and SOI.

The link between all three variable realms – CO_2, SOI and temperature – can be further observed in Fig. 7 and Table 7. Figure 7 shows SOI, second-difference atmospheric CO_2 and first-difference temperature, each of the latter two series phase-shifted for maximum correlation with SOI (as in Table 5). Looking at priority, Table 6 shows that maximum correlation occurs when second-difference CO_2 leads SOI. It is also noted that the correlation coefficients for the correlations between the curves shown in Table 6 have all converged in value compared to those shown in Table 5.

Looking at the differences between the curves shown in Fig. 7, two of the major departures between the curves coincide with volcanic aerosols – from the El Chichon volcanic eruption in 1982 and the Pinatubo eruption in 1992 (Lean and Rind, 2009). With these volcanism-related factors taken into account, it is notable (when expressed in the form of the transformations in Fig. 7) that the signatures of all three

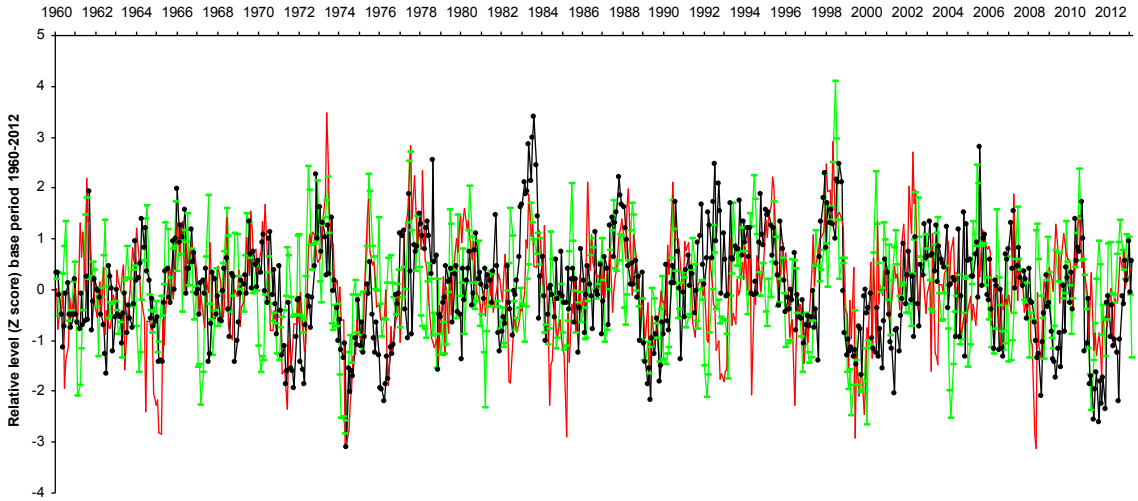

Figure 7. Z-scored monthly data from 1960-2012: sign-reversed SOI (unsmoothed and neither led nor lagged) (dotted black curve); second-difference CO_2 smoothed by 2×13 month moving average and led relative to SOI by 2 months (green dashed curve); and first-difference global surface temperature smoothed by a 13-month moving average and led by 3 months (red curve).

Table 7. OLS dynamic regression between second-difference atmospheric CO_2 and reversed Southern Oscillation Index for monthly data for the period 1959–2012, with autocorrelation taken into account.

Independent variable/s[a]	Dependent variable[a]	Independent variable regression coefficients	Independent variable p value	Whole model adjusted R-squared	Whole model p value	LM test for autocorrelation[b]
Led3m2x13mma 1stDiffCO_2	ReverseSOI	0.07699	< 0.011	0.478	1.80×10^{-89}	0.214
Led1mReverseSOI		0.456	< 0.00001			
Led2mreverseSOI		0.272	< 0.00001			

[a] Z-scored. [b] Whole model: LM test for autocorrelation up to order 12 – null hypothesis: no autocorrelation.

curves are so essentially similar that it is almost as if all three curves are different versions of – or responses to – the same initial signal.

So, a case can be made that first- and second-difference CO_2 and temperature and SOI respectively all reflect different aspects of the same process.

4.2.2 Time series analysis

We now assess more formally the relationship between second-difference CO_2 and SOI. As for first-difference CO_2 and temperature above, stationarity has been established. Again, there is statistically significant autocorrelation at lags of 1 and 2 months, leading to an overall Breusch–Godfrey test statistic (LMF) of 126.9, with p value $= P(F(12, 626) > 126.901) = 1.06 \times 10^{-158}$.

Table 7 shows the results of a dynamic model with the dependent variable used at each of the two lags as further independent variables; there is now no statistically significant autocorrelation which has not been accounted for.

As Table 7 shows, a highly statistically significant model has been established. As for temperature, it shows that the SOI in a given period is strongly influenced by the SOI of closely preceding periods. Again as for temperature, it provides evidence that there is a clear role in the model for second-difference CO_2.

With this established, it is noted that while the length of series in the foregoing analysis was limited by the start date of the atmospheric CO_2 series (January 1958), high temporal resolution (monthly) SOI data go back considerably further, to 1877. This long period SOI series (for background see Troup, 1965) is that provided by the Australian Bureau of Meteorology, sourced here from the Science Delivery Division of the Department of Science, Information Technology, Innovation and the Arts, Queensland, Australia. As equivalent temperature data are also available (the global surface temperature series already used above (HadCRUT4) goes back as far as 1850), these two longer series are now plotted in Fig. 8. Notable is the continuation of the striking similarity between the two signatures already shown in Fig. 7 over this longer period.

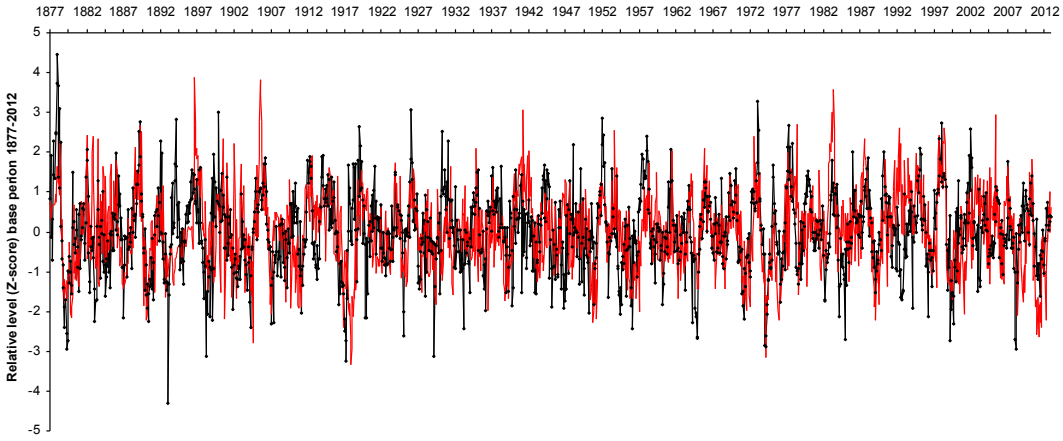

Figure 8. *Z*-scored monthly data from 1877–2012: sign-reversed SOI (unsmoothed and neither led nor lagged) (red curve); and first-difference global surface temperature smoothed by a 13-month moving average and led relative to SOI by 3 months (black dotted curve).

Table 8. OLS dynamic regression between first-difference global surface temperature and reversed Southern Oscillation Index for monthly data for the period 1877–2012, with autocorrelation taken into account.

Independent variable/s[a]	Dependent variable[a]	Independent variable regression coefficients	Independent variable *p* value	Whole model adjusted *R*-squared	Whole model *p* value	LM test for autocorrelation[b]
Led3m12mma1stDiffTEMP	ReverseSOI	0.140	< 0.00001	0.466	3.80×10^{-221}	0.202
Led1mReverseSOI		0.465	< 0.00001			
Led2mReverseSOI		0.210	< 0.00001			

[a] *Z*-scored. [b] Whole model: LM test for autocorrelation up to order 3 – null hypothesis: no autocorrelation.

Turning to regression analysis, as previously the Breusch–Godfrey procedure shows that for lags up to lag 12, the majority of autocorrelation is again restricted to the first two lags. Table 8 shows the results of a dynamic model with the dependent variable used at each of the two lags as further independent variables.

In comparison with Table 7, the extended time series modelled in Table 8 shows a remarkably similar *R*-squared statistic: 0.466 compared with 0.478. By contrast, the partial regression coefficient for second-difference CO_2 has increased, to 0.14 compared with 0.077. It is beyond the scope of this study, but the relationship of SOI and second-difference CO_2 means it is now possible to produce a proxy for monthly atmospheric CO_2 from 1877 – a date approximately 75 years prior to the start of the CO_2 monthly instrumental record in January 1958.

4.2.3 Granger causality analysis

This section assesses whether second-difference CO_2 can be considered to Granger-cause SOI. This assessment is carried out using data for the period 1959 to 2012.

Results of stationarity tests for each series are given in Table 9. Each series is shown to be stationary. These results imply that we can approach the issue of possible Granger causality by using a conventional VAR model, in the levels of the data, with no need to use a "modified" Wald test (as used in the Toda and Yamamoto (1995) methodology).

Table 9. Augmented Dickey–Fuller (ADF) test for stationarity for monthly data 1959–2012 for second-difference CO_2 and sign-reversed SOI.

	ADF statistic	*p* value	Test interpretation
Second-difference CO_2	−10.077	0.000	Stationary
Sign-reversed SOI	−6.681	0.000	Stationary

Simple OLS regressions of SOI against separate lagged values of second-difference CO_2 (including an intercept) confirm the finding that the highest correlation is when a two-period lag is used.

A two-equation VAR model is needed for reverse-sign SOI and second-difference CO_2. Using SIC, the optimal maximum lag length is found to be 2 lags. When the VAR model is estimated with this lag structure (Table 10), testing the null hypothesis that there is no serial correlation at lag order h,

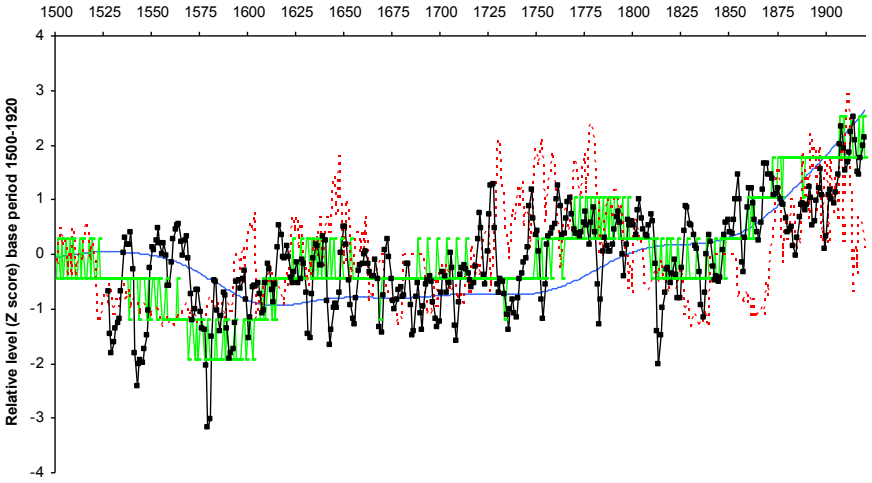

Figure 9. *Z*-scored annual data: paleoclimate time series from 1500: ice core level of CO_2 (blue curve), level of CO_2 transformed into first-difference form (green barred curve); and temperature from speleothem (red dashed curve) and tree ring data (black boxed curve).

Table 10. VAR Residual Serial Correlation LM Tests component of Granger causality testing of relationship between second-difference CO_2 and SOI. Initial 2-lag model.

Lag order	LM-Stat	*p* value*
1	10.62829	0.0311
2	9.71675	0.0455
3	2.948737	0.5664
4	9.711391	0.0456
5	10.67019	0.0305
6	37.13915	0
7	1.268093	0.8668

* *p* values from chi-square with 4 df.

shows that there is evidence of autocorrelation in the residuals.

This suggests that the maximum lag length for the variables needs to be increased. The best results (in terms of lack of autocorrelation) were found when the maximum lag length is 3. (Beyond this value, the autocorrelation results deteriorated substantially, but the conclusions below, regarding Granger causality, were not altered.)

Table 11 shows that the preferred, 3-lag model, still suffers a little from autocorrelation. However, as we have a relatively large sample size, this will not impact adversely on the Wald test for Granger causality.

The relevant EViews output from the VAR model is entitled VAR Granger causality/block exogeneity Wald tests and documents the following summary results – Wald Statistic (*p* value): null depicts that there is no Granger causality from second-difference CO_2 to sign-reversed SOI; Chi-Square 22.554 (p value = 0.0001).

The forgoing Wald statistic shows that the null hypothesis is strongly rejected – in other words, there is very strong evidence of Granger causality from second-difference CO_2 to sign-reversed SOI.

4.3 Palaeoclimate data

So far, the time period considered in this study has been pushed back in the instrumental data realm to 1877. If non-instrumental paleoclimate proxy sources are used, CO_2 data now at annual frequency can be taken further back. The following example uses CO_2 and temperature data. The temperature reconstruction used here commences in 1500 and is that of Frisia et al. (2003), derived from annually laminated speleothem (stalagmite) records. A second temperature record (Moberg et al., 2005) is from tree ring data. The atmospheric CO_2 record (Robertson et al., 2001) is from fossil air trapped in ice cores and from instrumental measurements. The trends for these series are shown in Fig. 9.

Visual inspection of the figure shows that there is a strong overall likeness in signature between the two temperature series, and between them and first-difference CO_2. The similarity of signature is notably less with level of CO_2. It can be shown that level of CO_2 is not stationary and, even with the two other series which are stationary, the strongly smoothed nature of the temperature data makes removal of the autocorrelation impossible. Nonetheless, noting that data uncorrected for autocorrelation still provide valid correlations (Greene, 2012) – only the statistical significance is uncertain – it is simply noted that first-difference CO_2 displays a better correlation with temperature than level of CO_2 for each temperature series (Table 12).

4.4 Normalized Difference Vegetation Index (NDVI)

Using the Normalized Difference Vegetation Index (NDVI) time series as a measure of the activity of the land biosphere, this section now investigates the land biosphere as a candi-

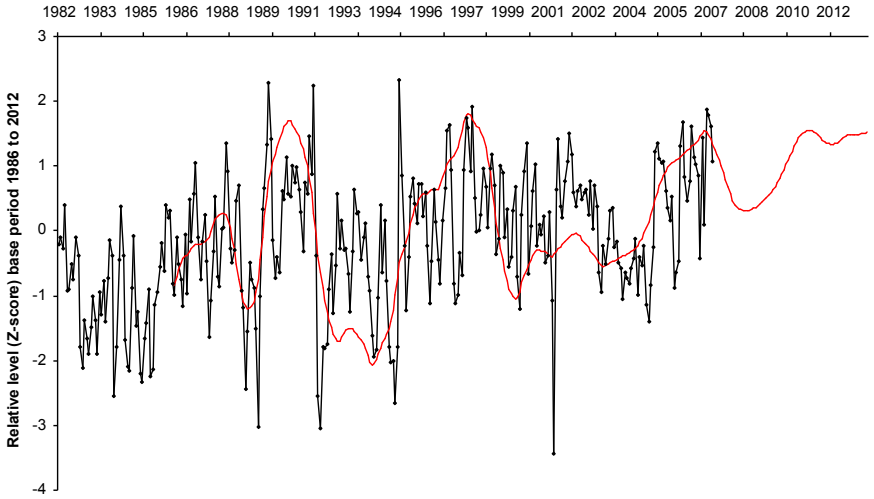

Figure 10. Z-scored monthly data: NDVIG (black dotted curve) compared to NDVIV (red curve).

Table 11. VAR Residual Serial Correlation LM Tests component of Granger causality testing of relationship between second-difference CO_2 and SOI. Preferred 3-lag model.

Lag order	LM-Stat	p value*
1	1.474929	0.8311
2	4.244414	0.3739
3	2.803332	0.5913
4	13.0369	0.0111
5	8.365221	0.0791
6	40.15417	0
7	1.698265	0.791

* p values from chi-square with 4 df.

date mechanism for the issue, identified in the Introduction, of the increasing difference between the observed global surface temperature trend and that suggested by general circulation climate models.

The trend in the terrestrial CO_2 sink is estimated annually as part of the assessment of the well-known global carbon budget (Le Quéré et al., 2014). It is noted that there is a risk of circular argument concerning correlations between the terrestrial CO_2 sink and interannual (first-difference) CO_2 because the terrestrial CO_2 sink is defined as the residual of the global carbon budget (Le Quéré et al., 2014). By contrast, the Normalized Difference Vegetation Index (NDVI) involves direct (satellite-derived) measurement of terrestrial plant activity. For this reason and because, of the two series, only NDVI is provided in monthly form, we will use only NDVI in what follows.

Table 12. Correlations (R) between paleoclimate CO_2 and temperature estimates 1500–1940.

	Temperature (speleothem)	Temperature (tree ring)
Level of CO_2 (ice core)	0.369	0.623
First diff. CO_2 (ice core)	0.558	0.721

4.4.1 Preparation of the global NDVI series used in this paper

Globally aggregated GIMMS NDVI data from the Global Land Cover Facility site are available from 1980 to 2006. This data set is referred to here as NDVIG. Spatially disaggregated GIMMS NDVI data from the GLCF site is available from 1980 to the end of 2013. An analogous global aggregation of this spatially disaggregated GIMMS NDVI data – from 1985 to end 2013 – was obtained from the Institute of Surveying, Remote Sensing and Land Information, University of Natural Resources and Life Sciences, Vienna. This data set is labelled NDVIV.

Pooling the two series enabled the longest time span of data aggregated at global level. The two series were pooled as follows. Figure 10 shows the appearance of the two series. Each series is Z-scored by the same common period of overlap (1985–2006). The extensive period of overlap can be seen, as can the close similarity in trend between the two series. The figure also shows that the seasonal adjustment smoothings vary between the two series. Seasonality was removed for the NDVIV series using the 13-month moving average smoothing used throughout this paper. This required two passes using the 13-month moving average (2×13), which leads to a smoother result than seen for the NDVIG series.

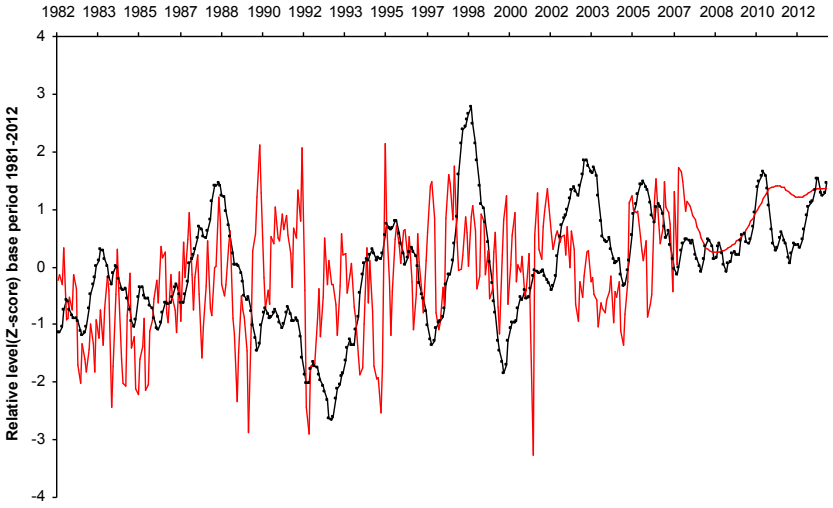

Figure 11. Z-scored monthly data: NDVI (black curve) compared to the difference between the temperature projected from an IPCC mid-range scenario model (CMIP3, SRESA1B scenario) run for the IPPC fourth assessment report (IPCC, 2007) and global surface temperature (red dotted curve).

Table 13. Order of integration test results for NDVI series for monthly data from 1981–2012. The Schwartz information criterion (SIC) was used to select an optimal maximum lag length in the tests.

NDVI series	Null hypothesis: the series has a unit root	Probability of unit root
NDVIV	Lag length: 16 (Automatic – based on SIC, maxlag = 16)	0.0122
NDVIG	Lag length: 1 (Automatic – based on SIC, maxlag = 15)	7.23×-14
NDVIGV	Lag length: 1 (Automatic – based on SIC, maxlag = 16)	4.18×10^{-16}

Pretis and Hendry (2013) observe that pooling data (i) from very different measurement systems and (ii) displaying different behaviour in the sub-samples can lead to errors in the estimation of the level of integration of the pooled series.

The first risk of error (from differences in measurement systems) is overcome here as both the NDVI series are from the same original disaggregated data set. The risk associated with the sub-samples displaying different behaviour and leading to errors in levels of integration is considered in the following section by assessing the order of each input series separately, and then the order of the pooled series.

Table 13 provides order of integration test results for the three NDVI series. The analysis shows all series are stationary ($I(0)$). It is, therefore, valid to pool the two series. Pooling was done by appending the Z-scored NDVIV data to the Z-scored NDVIG data at the point where the Z-scored NDVIG data ended (in the last month of 2006).

As discussed in the Introduction, Fig. 1 shows that since around the year 2000 there is an increasing difference between the temperature projected by a mid-level IPCC model and that observed. Any cause for this increasing difference must itself show an increase in activity over this period.

The purpose of this section is, therefore: (i) to derive an initial simple indicative quantification of the increasing difference between the temperature model and observation; and (ii) to assess whether global NDVI is increasing. If NDVI is increasing, this is support for NDVI being a candidate for the cause of the temperature model–observation difference. If there is a statistically significant relationship between the two increases, this is further support for NDVI being a candidate for the cause of the model–observation difference, and hence worthy of further detailed research. A full analysis of this question is beyond the scope of the present paper.

4.4.2 Preparation of the indicative series for the difference between the temperature projected from a mid-level IPCC model and that observed

A simple quantification of the difference between the temperature projected from a mid-level IPCC model and that observed can be derived by subtracting the (Z-scored) temperature projected from the IPCC mid-range scenario model (CMIP3, SRESA1B scenario run for the IPCC fourth assessment report; IPCC, 2007) shown in Fig. 1, from the observed global surface temperature also shown in Fig. 1. This quantification is depicted in Fig. 11 for monthly data and, to re-

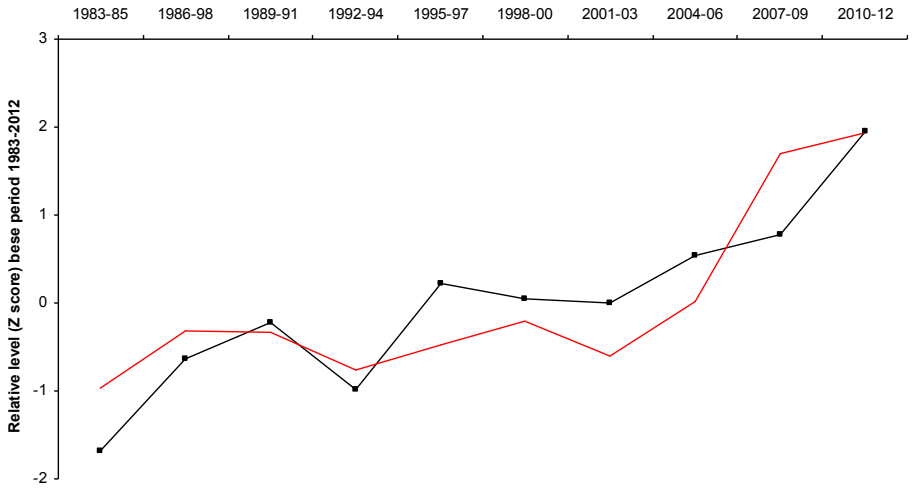

Figure 12. *Z*-scored data for periods each of 36 months, averaged: NDVI (black curve) compared to the difference between the temperature projected from an IPCC mid-range scenario model (CMIP3, SRESA1B scenario) run for the IPPC fourth assessment report (IPCC, 2007) and global surface temperature (red dotted curve).

duce the influence of noise and seasonality, in Fig. 12 for the same data pooled into 3-year bins.

4.4.3 Comparison of the pooled NDVI series with the difference between projected and observed global surface temperature

Figure 11, displaying monthly data, compares NDVI with the difference between the temperature projected from an IPCC mid-range scenario model (CMIP3, SRESA1B scenario run for the IPPC fourth assessment report; IPCC, 2007) and global surface temperature (red dotted curve). Both curves rise in more recent years.

The trends for the 36-month pooled data in Fig. 12 show considerable commonality. OLS regression analysis of the relationship between the curves in Fig. 12 shows that the best fit between the curves involves no lead or lag. The correlation between the curves displays an adjusted R-squared value of 0.86. This is statistically significant ($p = 0.00185$). As expected with such aggregated multi-year data, the relationship shows little or no autocorrelation (test statistic: LMF = 1.59 with p value = $P(F(5,3) > 1.59) = 0.37$). The similarity between the trend in the NDVI and the difference between IPCC temperature modelling and observed temperature is evidence supporting the possibility that the NDVI may contribute to the observed global surface temperature departing from the IPCC modelling.

5 Discussion

The results in this paper show that there are clear links at the highest standard of non-experimental causality – that of Granger causality – between first- and second-difference CO_2 and the major climate variables of global surface temperature and the Southern Oscillation Index, respectively.

Relationships between first- and second-difference CO_2 and climate variables are present for all the timescales studied, including temporal start points situated as long ago as 1500. In the instances where time-series analysis accounting for autocorrelation could be successfully conducted, the results were always statistically significant. For the further instances (for those studies using data series commencing before 1877) the data were not amenable to time-series analysis – and therefore also not amenable to testing for Granger causality – due to the strongly smoothed nature of the temperature data available which made removal of the autocorrelation impossible (see Sect. 4.3). Nonetheless, the scale of the non-corrected correlations observed was of the same order of magnitude as those of the instances that were able to be corrected for autocorrelation.

Given the timescales over which these effects are observed, the results taken as a whole clearly suggest that the mechanism observed is long-term, and not, for example, a creation of the period of the steepest increase in anthropogenic CO_2 emissions, a period which commenced in the 1950s (IPCC 2014).

Taking autocorrelation fully into account in the time-series analyses demonstrates the major role of immediate past instances of the dependent variable (temperature, and SOI) in influencing its own present state. This was found in all cases where time-series models could be prepared. This was not to detract from the role of first- and second-difference CO_2 – in all relevant cases, they were significant in the models as well.

According to Mudelsee (2010) and Wilks (2011), such autocorrelation in the atmospheric sciences (also called persistence or "memory") is characteristic of many types of climatic fluctuations.

In the specific case of the temperature and first-difference CO_2 relationship, the significant autocorrelation for temperature occurred with present temperature being affected by the immediately prior month and the month before that. As mentioned above, for atmospheric CO_2 and global surface temperature, others (Sun and Wang, 1996; Triacca, 2005; Kodra et al., 2011; Attanasio and Triacca, 2011; Attanasio et al., 2013; Stern and Kaufmann, 2014) have conducted Granger causality analyses involving the use of lags of both dependent and independent variables. These studies, however, are not directly comparable with the present study. Firstly, while reporting the presence or absence of Granger causality, the studies did not report lead or lag information. Secondly, the studies used annual data, so could not investigate the dynamics of the relationships at the interannual (monthly) level where our findings were greatest.

The anthropogenic global warming (AGW) hypothesis has two main dimensions (IPCC, 2007; Pierrehumbert, 2011): (i) that increasing CO_2 causes increasing atmospheric temperature (via a radiative forcing mechanism) and (ii) that most of the increase in atmospheric CO_2 in the last hundred years has been due to human causes – a result of accelerated release of CO_2 from the burning of fossil fuels. The evidence for this (Levin and Hesshaimer, 2000) comes from the analysis of changes in the proportion of carbon isotopes in tree rings from the past two centuries.

The results presented in this paper are supportive of the AGW hypothesis for two reasons: firstly, increasing atmospheric CO_2 is shown to drive increasing temperature; and secondly, the results deepen the evidence for a CO_2 influence on climate in that second-difference CO_2 is shown to drive the SOI.

The difference between this evidence for the effect of CO_2 on climate and that from the majority of GCM simulations is that in the simulations, the temperature rises roughly linearly with atmospheric CO_2, whereas the present results show that the climate effects result from persistence of previous effects and from *change* in the level of CO_2.

On the face of it, then, this model seems to leave little room for the linear radiative forcing aspect of the AGW hypothesis. However more research is needed in this area.

Reflection on Fig. 1 shows that the radiative mechanism would be supported if a second mechanism existed to cause the difference between the temperature projected for the radiative mechanism and the temperature observed. The observed temperature would then be seen to result from the addition of the effects of these two mechanisms.

As discussed in the Introduction, Hansen et al. (2013) have suggested that the mechanism for the pause in the global temperature increase since 1998 may be the planetary biota, in particular the terrestrial biosphere. As an initial indicative quantified characterisation of this possibility, Sect. 4.4 derived a simple measure of the increasing difference between the global surface temperature trend projected from a mid-range scenario climate model and the observed trend. This depiction of the difference displayed a rising trend. The time-series trend for the globally aggregated Normalized Difference Vegetation Index – which represents the changing levels of photosynthetic activity of the terrestrial biosphere – was also presented. This was shown also to display a rising trend.

If by further research, for example by Granger causality analysis, the global vegetation can be shown to embody the second mechanism, this would be evidence that the observed global temperature does result from the effects of two mechanisms in operation together – the radiative, level-of-CO_2 mechanism, with the biological first-difference-of-CO_2 mechanism.

Hence the biosphere mechanism would supplement, rather than replace, the radiative mechanism.

Further comprehensive time-series analysis of the NDVI data and relevant climate data, beyond the scope of the present paper, could throw light on these questions.

The Supplement related to this article is available online at doi:10.5194/acp-15-11571-2015-supplement.

Acknowledgements. The authors would like to acknowledge with appreciation the support and advice of J. Gordon and C. Dawson, and the comments of the two anonymous referees of the paper which we consider to have improved it markedly.

Edited by: R. MacKenzie

References

Adams, J. M. and Piovesan, G.: Long series relationships between global interannual CO_2 increment and climate: Evidence for stability and change in role of the tropical and boreal-temperate zones, Chemosphere, 59, 1595–1612, 2005.

Attanasio, A. and Triacca, U.: Detecting human influence on climate using neural networks based Granger causality, Theor. Appl. Climatol., 103, 103–107, 2011.

Attanasio, A., Pasini, A., and Triacca, U.: Granger causality analyses for climatic attribution, Atmospheric and Climate Sciences, 3, 515–522, 2013.

Bacastow, R. B.: Modulation of atmospheric carbon dioxide by the southern oscillation, Nature, 261, 116–118, 1976.

Banerjee, A., Dolado, J., Galbraith, J. W., and Hendry, D. F.: Co-integration, error-correction, and the econometric analysis of non-stationary data, Oxford University Press, Oxford, 1993.

Barichivich, J., Briffa, K. R., Myneni, R. B., Osborn, T. J., Melvin, T. M., Ciais, P., Piao, S., and Tucker, C.: Large-scale variations in the vegetation growing season and annual cycle of atmospheric CO_2 at high northern latitudes from 1950 to 2011, Glob. Change Biol., 19, 3167–3183, 2013.

Beenstock, M., Reingewertz, Y., and Paldor, N.: Polynomial cointegration tests of anthropogenic impact on global warming, Earth Syst. Dynam., 3, 173–188, doi:10.5194/esd-3-173-2012, 2012.

Bellenger, H., Guilyardi, E., Leloup, J., Lengaigne, M., and Vialard, J.: ENSO representation in climate models: from CMIP3 to CMIP5, Clim. Dynam., 42, 1999–2018, 2014.

Breitung, J. and Swanson, N. R.: Temporal aggregation and spurious instantaneous causality in multiple time series models, J. Time Ser. Anal., 23, 651–665, 2002.

Canty, T., Mascioli, N. R., Smarte, M. D., and Salawitch, R. J.: An empirical model of global climate – Part 1: A critical evaluation of volcanic cooling, Atmos. Chem. Phys., 13, 3997–4031, doi:10.5194/acp-13-3997-2013, 2013.

Chen, X. and Tung, K.: Varying planetary heat sink led to global-warming slowdown and acceleration, Science 345, 897–903, doi:10.1126/science.1254937, 2014.

Christriano, L. J. and Eichenbaum, M.: Temporal aggregation and structural inference in macroeconomics, Carnegie-Rochester Conference Series on Public Policy, 26, 63–130, 1987.

Cowtan, K. and Way, R. G.: Coverage bias in the HadCRUT4 temperature series and its impact on recent temperature trends, Q. J. Roy. Meteor. Soc., 140, 1935–1944, 2014.

Denman, K. L., Brasseur, G., Chidthaisong, G., Ciais, A., Cox, P. P. M., Dickinson, P. M., Hauglustaine, R. E., Heinze, D., Holland, C. E, Jacob, D., Lohmann, U., Ramachandran, S., da Silva Dias, P. L., Wofsy, S. C., and Zhang, X.: Couplings between changes in the climate system and biogeochemistry, Climate Change 2007: The physical science basis. Contribution of working group I to the fourth assessment report of the intergovernmental panel on climate change, edited by: Solomon, S., Qin, D., Manning, M., Chen, Z., Marquis, M., Avery, K. B., Tignor, M., and Miller, H. L., Cambridge University Press, Cambridge, United Kingdom and New York, NY, USA, 2007.

Dickey, D. A. and Fuller, W. A.: Distribution of the estimators for autoregressive time series with a unit root, J. Am. Stat. Assoc., 74, 427–431, 1979.

Dickey, D. A. and Fuller, W. A.: Likelihood ratio statistics for autoregressive time series with a unit root, Econometrica, 49, 1057–1072, 1981.

Diebold, F. X.: Discussion: Effect of seasonal adjustment filters on tests for a unit root, J. Econometrics, 55, 99–103, 1993.

Dieleman, W. I. J., Vicca, S., Dijkstra, F. A., Hagedorn, F., Hovenden, M. J., Larsen, K. S., Morgan, J. A., Volder, A., Beier, C., Dukes, J. S., King, J., Leuzinger, S., Linder, S., Luo, Y., Oren, R., De Angelis, P., Tingey, D., Hoosbeek, M. R., and Janssens, I. A.: Simple additive effects are rare: a quantitative review of plant biomass and soil process responses to combined manipulations of CO_2 and temperature, Glob. Change Biol., 18, 2681–2693, 2012.

Ding, M., Chen, Y., and Bressler, S. L.: Granger causality: Basic theory and applications to neuroscience, in: Handbook of Time Series Analysis, edited by: Schelter, B., Winterhalder, M., and Timmer, J., Wiley-VCH Verlag, Weinhem, 437–460, 2006.

Dufour, J.-M. and Renault, E.: Short run and long run causality in time series: theory, Econometrica, 66, 1099–1125, 1998.

Elliott, G., Rothenberg, T. J., and Stock, J. H.: Efficient tests for an autoregressive unit root, Econometrica, 64, 813–836, 1996.

Folland, C. K., Colman, A. W., Smith, D. M., Boucher, O., Parker, D. E., and Vernier, J. P.: High predictive skill of global surface temperature a year ahead, Geophys. Res. Lett., 40, 761–767, 2013.

Foster, G. and Rahmstorf, S.: Global temperature evolution 1979–2010, Environ. Res. Lett., 6, 044022, doi:10.1088/1748-9326/6/4/044022, 2011.

Franses, P. H.: Moving average filters and unit roots, Econ. Lett., 37, 399–403, 1991.

Frisia, S., Borsato, A., Preto, N., and McDermott, F.: Late Holocene annual growth in three Alpine stalagmites records the influence of solar activity and the North Atlantic Oscillation on winter climate, Earth Planet. Sc. Lett., 216, 411–424, 2003.

Fyfe, J. C. and Gillett, N. P.: Recent observed and simulated warming, Nature Climate Change, 4, 150–151, 2014.

Fyfe, J. C., Gillett, N. P, and Zwiers, F. W.: Overestimated global warming over the past 20 years, Nature Climate Change, 3, 767–769, 2013.

Geweke, J.: Measures of conditional linear dependence and feedback between time series, J. Am. Stat. Assoc., 79, 907–915, 1984.

Ghosh, S. and Rao, C. R. (Eds.): Design and Analysis of Experiments, Handbook of Statistics, 13, North-Holland, 1996.

Ghysels, E.: Unit root tests and the statistical pitfalls of seasonal adjustment: The case of U.S. postwar real gross national product, Journal of Business and Economic Statistics, 8, 145–152, 1990.

Ghysels, E. and Perron, P.: The effect of seasonal adjustment filters on tests for a unit root, J. Econometrics, 55, 57–98, 1993.

Granger, C. W. J.: Investigating causal relations by econometric models and cross-spectral methods, Econometrica, 37, 424–438, 1969.

Greene, W. H.: Econometric Analysis, 7th Edn., Prentice Hall, Boston, 2012.

Gribbons, B. and Herman, J.: True and quasi-experimental designs, Practical Assessment, Research and Evaluation, 5, available at: http://PAREonline.net/getvn.asp?v=5&n=14 (last access: 14 October 2015), 1997.

Guemas, V., Doblas-Reyes, F. J., Andreu-Burillo, I., and Asif, M.: Retrospective prediction of the global warming slowdown in the past decade, Nature Climate Change, 3, 649–653, 2013.

Guilyardi, E., Bellenger, H., Collins, M., Ferrett, S., Cai, W., and Wittenberg, A.: A first look at ENSO in CMIP5, Clivar. Exch., 17, 29–32, 2012.

Gulasekaran, R. and Abeysinghe, T.: The distortionary effects of temporal aggregation on Granger causality, Working Paper No. 0204, Department of Economics, National University of Singapore, 2002.

Hansen, J., Kharecha, P., and Sato, M.: Climate forcing growth rates: doubling down on our Faustian bargain, Environ. Res. Lett., 8, 011006, doi:10.1088/1748-9326/8/1/011006, 2013.

Hidalgo, F. and Sekhon, J.: Causality, in: International encyclopedia of political science, edited by: Badie, B., Berg-Schlosser, D., and Morlino, L., 204–211, 2011.

Holbrook, N. J. Davidson, J., Feng, M., Hobday, A. J., Lough, J. M., McGregor, S., and Risbey, J. S.: El niño-southern oscillation, in: A marine climate change impacts and adaptation report card for Australia 2009, edited by: Poloczanska, E. S., Hobday, A. J., and Richardson, A. J., NCCARF Publication, 05/09, 2009.

Hume, D.: An enquiry into human understanding, cited in: Hidalgo and Sekhon (2011), 1751.

Hyndman, R. J.: Moving averages, in: International encyclopedia of statistical science, edited by: Lovirc, M., 866–869, Springer, New York, 2010.

IHS EViews: EViews 7.2, IHS Global Inc., Irvine, California, 2011.

Imbers, J., Lopez, A., Huntingford, C., and Allen, M. R.: Testing the robustness of the anthropogenic climate change detection statements using different empirical models, J. Geophys. Res.-Atmos., 118, 3192–3199, 2013.

IPCC: Climate Change 2007: The physical science basis. Contribution of working group I to the fourth assessment report of the intergovernmental panel on climate change, edited by: Qin, D., Manning, M., Chen, Z., Marquis, M., Avery, K. B., Tignor, M., and Miller, H. L., Cambridge University Press, Cambridge, United Kingdom and New York, NY, USA, 2007.

IPCC: Climate Change 2013: The Physical Science Basis. Contribution of Working Group I to the Fifth Assessment Report of the Intergovernmental Panel on Climate Change, edited by: Stocker, T. F., Qin, D., Plattner, G.-K., Tignor, M., Allen, S. K., Boschung, J., Nauels, A., Xia, Y., Bex, V., and Midgley, P. M., Cambridge University Press, Cambridge, United Kingdom and New York, NY, USA, 1535 pp., 2014.

Karl, T. R., Arguez, A., Huang, B., Lawrimore, J. H., McMahon, J. R., Menne, M. J., Peterson, T. C., Vose, R. S., and Zhang, H.-M.: Possible artifacts of data biases in the recent global surface warming hiatus, Science, 348, 1469–1472, 2015.

Kaufmann, R. K., Kauppi, H., and Stock, J. H.: Emissions, concentrations, and temperature: a time series analysis, Climatic Change, 77, 249–278, 2006.

Keeling, R. F., Piper, S. C., Bollenbacher, A. F., and Walker, S. J.: Carbon Dioxide Research Group, Scripps Institution of Oceanography (SIO), University of California, La Jolla, California USA 92093-0444, available at: http://cdiac.ornl.gov/ftp/trends/co2/maunaloa.co2 (last access: 14 July 2014), 2009.

Kiviet, J. F.: On the rigour of some misspecification tests for modelling dynamic relationships, Rev. Econ. Stud., 53, 241–261, 1986.

Kodra, E., Chatterjee, S., and Ganguly, A. R.: Exploring Granger causality between global average observed time series of carbon dioxide and temperature, Theor. Appl. Climatol., 104, 325–335, 2011.

Kopp, G. and Lean, J. L.: A new, lower value of total solar irradiance: evidence and climate significance, Geophys. Res. Lett., 38, L01706, doi:10.1029/2010GL045777, 2011.

Kosaka, Y. and Shang-Ping, X.: Recent global-warming hiatus tied to equatorial Pacific surface cooling, Nature, 501, 403–407, doi:10.1038/nature12534, 2013.

Kuo, C., Lindberg, C., and Thomson, D. J.: Coherence established between atmospheric carbon dioxide and global temperature, Nature, 343, 709–714, 1990.

Lean, J. L. and Rind, D. H.: How natural and anthropogenic influences alter global and regional surface temperatures: 1889 to 2006, Geophys. Res. Lett., 35, L18701, doi:10.1029/2008GL034864, 2008.

Lean, J. L. and Rind, D. H.: How will Earth's surface temperature change in future decades?, Geophys. Res. Lett., 36, L15708, doi:10.1029/2009GL038932, 2009.

Le Quéré, C., Peters, G. P., Andres, R. J., Andrew, R. M., Boden, T. A., Ciais, P., Friedlingstein, P., Houghton, R. A., Marland, G., Moriarty, R., Sitch, S., Tans, P., Arneth, A., Arvanitis, A., Bakker, D. C. E., Bopp, L., Canadell, J. G., Chini, L. P., Doney, S. C., Harper, A., Harris, I., House, J. I., Jain, A. K., Jones, S. D., Kato, E., Keeling, R. F., Klein Goldewijk, K., Körtzinger, A., Koven, C., Lefèvre, N., Maignan, F., Omar, A., Ono, T., Park, G.-H., Pfeil, B., Poulter, B., Raupach, M. R., Regnier, P., Rödenbeck, C., Saito, S., Schwinger, J., Segschneider, J., Stocker, B. D., Takahashi, T., Tilbrook, B., van Heuven, S., Viovy, N., Wanninkhof, R., Wiltshire, A., and Zaehle, S.: Global carbon budget 2013, Earth Syst. Sci. Data, 6, 235–263, doi:10.5194/essd-6-235-2014, 2014.

Levin, I. and Hesshaimer, V.: Radiocarbon – a unique tracer of global carbon cycle dynamics, Radiocarbon, 42, 69–80, 2000.

Lockwood, M.: Recent changes in solar outputs and the global mean surface temperature. III. Analysis of contributions to global mean air surface temperature rise, P. Roy. Soc. Math. Phy., 464, 1387–1404, 2008.

Marcellino, M.: Some consequences of temporal aggregation in empirical analysis, Journal of Business and Economic Statistics, 17, 129–136, 1999.

Meehl, G. A., Covey, C., Delworth, T., Latif, M., McAvaney, B., Mitchell, J. F. B., Stouffer, R. J., and Taylor, K. E.: The WCRP CMIP3 multi-model dataset: A new era in climate change research, B. Am. Meteorol. Soc., 88, 1383–1394, 2007.
CMIP3 data used available at: http://climexp.knmi.nl/data/itas_cmip3_ave_mean_sresa1b_0-360E_-90-90N_na.txt, last access: 10 June 2014.

Meehl, G. A., Arblaster, J. M., Fasullo, J. T. I., Hu, A., and Trenberth, K. E.: Model-based evidence of deep-ocean heat uptake during surface-temperature hiatus periods, Nature Climate Change, 1, 360–364, doi:10.1038/NCLIMATE1229, 2011.

Moberg, A., Sonechkin, D. M., Holmgren, K., Datsenko, N. M., and Karlén, W.: Highly variable Northern Hemisphere temperatures reconstructed from low- and high-resolution proxy data, Nature, 433, 613–617, 2005.

Morice, C. P., Kennedy, J. J., Rayner, N. A., and Jones, P. D.: Quantifying uncertainties in global and regional temperature change using an ensemble of observational estimates: the HadCRUT4 dataset, J. Geophys. Res., 117, D08101, doi:10.1029/2011JD017187, 2012.
HadCRUT4 data used available at: http://www.metoffice.gov.uk/hadobs/hadcrut4/data/current/time_series/HadCRUT.4.4.0.0.monthly_ns_avg.txt, last access: 12 September 2015.

Mudelsee, M.: Climate Time Series Analysis, Springer, Switzerland, 2010.

Olekalns, N.: Testing for unit roots in seasonally adjusted data, Econ. Lett., 45, 273–279, 1994.

Pankratz, A.: Forecasting with Dynamic Regression Models, Wiley, New York , 1991.

Pierrehumbert, R.: Infrared radiation and planetary temperature, Phys. Today, 64, 33–38, 2011.

Pretis, F. and Hendry, D. F.: Comment on "Polynomial cointegration tests of anthropogenic impact on global warming" by Beenstock et al. (2012) – some hazards in econometric modelling of climate change, Earth Syst. Dynam., 4, 375–384, doi:10.5194/esd-4-375-2013, 2013.

Robertson, A., Overpeck, J., Rind, D., Mosley-Thompson, D. E., Zielinski, G., Lean, J., Koch, D., Penner, J., Tegen, I., and Healy, R.: Hypothesized climate forcing time series for the last 500 years, J. Geophys. Res., 106, 14783–14803, doi:10.1029/2000JD900469, 2001.

Running, S. W., Nemani, R. R., Heinsch, F. A., Zhao, M., Reeves, M. C., and Hashimoto, H.: A continuous satellite-derived mea-

sure of global terrestrial primary production, BioScience, 54, 547–560, 2004.

Sato, M., Hansen, J. E., McCormick, M. P., and Pollack, J. B.: Stratospheric aerosol optical depths, 1850–1990, J. Geophys. Res., 98, 22987–22994, 1993.
Data used available at: http://data.giss.nasa.gov/modelforce/strataer/tau.line_2012.12.txt, last access: 10 August 2014.

Sims, C. A.: Distributed lag estimation when the parameter space is explicitly infinite, Dimensional. Ann. Math. Statist., 42, 1622–1636, 1971.

Stahle, D. W., D'Arrigo, R. D., Krusic, P. J., Cleaveland, M. K., Cook, E. R., Allan, R. J., Cole, J. E., Dunbar, R. B., Therrell, M. D., Gay, D. A., Moore, M. D., Stokes, M. A., Burns, B. T., Villanueva-Diaz, J., and Thompson, L. G.: Experimental dendroclimatic reconstruction of the Southern Oscillation, B. Am. Meteorol. Soc., 79, 2137–2152, 1998.

Stern, D. I. and Kander, A.: The role of energy in the industrial revolution and modern economic growth, CAMA Working Paper Series, Australian National University, 2011.

Stern, D. I. and Kaufmann, R. K.: Anthropogenic and natural causes of climate change, Climatic Change, 122, 257–269, doi:10.1007/s10584-013-1007-x, 2014.

Sun, L. and Wang, M.: Global warming and global dioxide emission: an empirical study, J. Environ. Manage., 46, 327–343, 1996.

Taylor, K. E., Stouffer, R. J., and Meehl, G. A.: An overview of CMIP5 and the experiment design, B. Am. Meteorol. Soc., 93, 485–498, doi:10.1175/BAMS-D-11-00094.1, 2012.
CMIP5 data used available at: http://climexp.knmi.nl/data/icmip5_tas_Amon_modmean_rcp45_0-360E_-90-90N_n_++ +a.txt, last access: 3 September 2015.

Toda, H. Y. and Yamamoto, T.: Statistical inferences in vector autoregressions with possibly integrated processes, J. Econometrics, 66, 225–250, 1995.

Triacca, U.: Is Granger causality analysis appropriate to investigate the relationship between atmospheric concentration of carbon dioxide and global surface air temperature?, Theor. Appl. Climatol., 81, 133–135, 2005.

Troup, A. J.: The Southern Oscillation, Q. J. Roy. Meteor. Soc., 91, 490–506, 1965.
SOI data used available at: https://www.longpaddock.qld.gov.au/seasonalclimateoutlook/southernoscillationindex/soidatafiles/MonthlySOI1887-1989Base.txt, last access: 25 August 2014.

Tucker, C. J., Pinzon, J. E., Brown, M. E., Slayback, D., Pak, E. W., Mahoney, R., Vermote, E., and El Saleous, N.: An extended AVHRR 8-km NDVI data set compatible with MODIS and SPOT vegetation NDVI data, Int. J. Remote Sens., 26, 4485–5598, 2005.

Wang, W., Ciais, P., Nemani, R. R., Canadell, J. G., Piao, S., Sitch, S., White, M. A., Hashimoto, H., Milesi, C., and Myneni, R. B.: Variations in atmospheric CO_2 growth rates coupled with tropical temperature, P. Natl. Acad. Sci. USA, 110, 13061–13066, 2013.

Wei, W. W. S.: The effect of systematic sampling and temporal aggregation on causality – a cautionary note, J. Am. Stat. Assoc., 77, 316–319, 1982.

Wilks, D. S.: Statistical methods in the atmospheric sciences: an introduction, Academic Press, London, 2011.

Zhang, Y., Guanter, L., Berry J. A., Joiner, J., van der Tol, C., Huete, A., Gitelson, A., Voigt, M., and Köhler, P.: Estimation of vegetation photosynthetic capacity from space-based measurements of chlorophyll fluorescence for terrestrial biosphere models, Glob. Change Biol., 20, 3727–3742, doi:10.1111/gcb.12664, 2014.

Zhou, J. and Tung, K.: Deducing multidecadal anthropogenic global warming trends using multiple regression analysis, J. Atmos. Sci., 70, 1–8, 2013.